Bull. Inst. Chem. Res., Kyoto Univ., Vol. 55, No. 2, 1977

Construction of Image Processing Systems and Application to the Random Noise Removal in Electron Micrographs

Masaki TSUJI, Seiji ISODA, Masayoshi OHARA, Ken-ichi KATAYAMA, and Keinosuke KOBAYASHI*

Received May 24, 1977

Computer and optical image processing systems were constructed to obtain high resolution images from electron micrographs. It seems that the main source of image degradation is the photographic graininess in electron-microscopic films. Spatial frequency filtering and linear integration are applied to the removal of random noises caused by the graininess of images. Signal-to-noise ratio is increased extremely in either processing. In particular, if both the periodic and the large scale irregular structures are required to be kept in processed images, spatial frequency filtering will be useful for the improvement in the signal-to-noise ratio.

I. INTRODUCTION

It is expected to improve the resolution of electron microscope (EM) up to the theoretical resolving limit[1] for the direct observation of molecular and atomic images. This expectation has never been fulfilled because of aberrations (in particular, the spherical aberration) of the objective lens in EM and the photographic graininess in electron-microscopic films (*e.g.*, granularity of photographic emulsion, the quantum noise of electron, *etc.*). In 1974, Kobayashi *et al.*[2] constructed the high resolution EM with a liquid helium specimen stage. With the small spherical aberration (C_s=1.2 mm), this EM should enable us to observe molecular or atomic images directly. The degradation of photographed images is, however, caused by the graininess. The graininess should be eliminated by means of image processing in preference to the correction of the effect of spherical aberration or defocus in order to obtain high resolution images.

The picture processing techniques have progressed in connection with the space research.[3] In these techniques, pictures are replaced into the mathematical images, and the picture processing techniques such as the geometric correction, the noise removal, the high frequency attenuation correction and so on are applied. For example these techniques have been applied to *a posteriori* image processing of electron micrographs, and became indispensable for the high resolving electron microscopy.[4~6] Thus a computer image processing system was constructed as a part of our high resolution EM study. Preliminary results were obtained by spatial frequency filtering and linear integration methods. A usual optical processing system was also constructed, and the results of image processing with this optical system are compared with those of the computer processing system.

* 辻　正樹，磯田正二，小原正義，片山健一，小林恵之助：Laboratory of Polymer Crystals, Institute for Chemical Research, Kyoto University, Uji, Kyoto.

II. CONSTRUCTION OF IMAGE PROCESSING SYSTEMS

Image processing methods for electron microscopy fall into two broad categories; (1) analogue and (2) digital processing. Although the apparatus for analogue processing (usually a purely optical method) is simple, this processing gives poor reproducibility and is quite unsatisfactory as quantitative processing. The system of digital processing (by means of a digital computer) is very complicated and requires much time to handle a large quantity of data. However this system shows good reproducibility and enables various kinds of processing with full accuracy.

Both analogue and digital processing methods were adopted in the present work and respective systems were constructed for image processing, especially for the removal of random noises caused by the photographic graininess in electron micrographs.

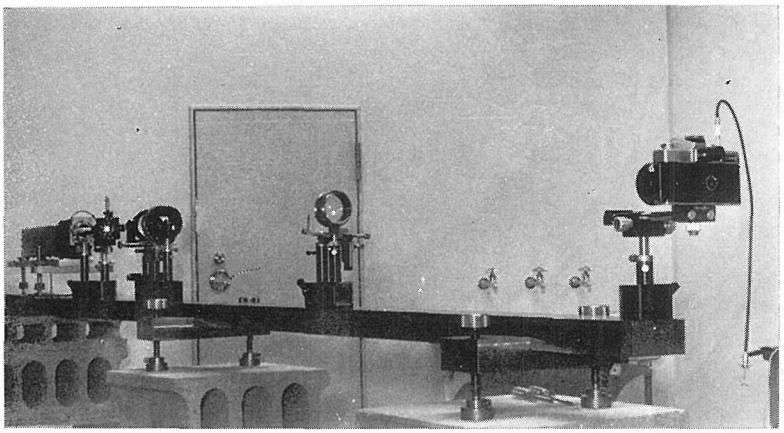

(a)

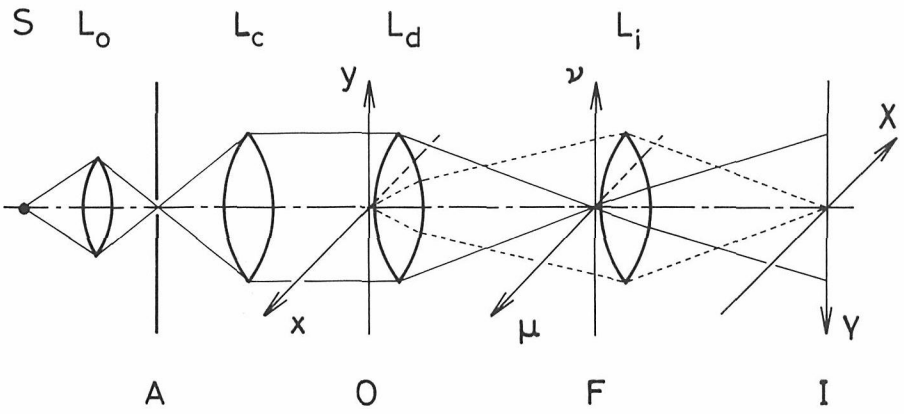

(b)

Fig. 1. Apparatus for optical filtering.
(a) General view.
(b) Schematic arrangement.
S; Light source (a He-Ne gas laser), L_o; Condenser lens, L_c; Collimating lens, L_d; Diffraction lens, L_i; Imaging lens, *A*; Aperture, *O*; Object plane, *F*; Back focal plane of lens L_d, *I*; Image plane.

II.1 Analogue Processing

The optical transform method developed by Taylor and Lipson[7] has been used for the anticipation and/or the interpretation of X-ray or electron diffraction pattern, and also for the analysis of an electron micrograph. On the basis of an optical transform principle, Klug *et al.*[4] have established the so-called optical filtering method for image processing of electron micrographs and applied this to the analysis of large biopolymer structures. Our apparatus for optical filtering was so constructed to remove random noises in electron micrographs. Figures 1(a) and 1(b) show a general view and a schematic arrangement of the apparatus, respectively.

The light beam from the source S (a He-Ne gas laser, the wavelength is 6328 Å) is focused at a point in the plane A by the lens L_o and passes through a diaphragm (20 μm in diameter). This point in the plane A is considered as an actual point source of light. The electron micrograph in the plane O is illuminated by the light waves collimated with the lens L_c. The Fourier spectrum of the object can be obtained in the back focal plane

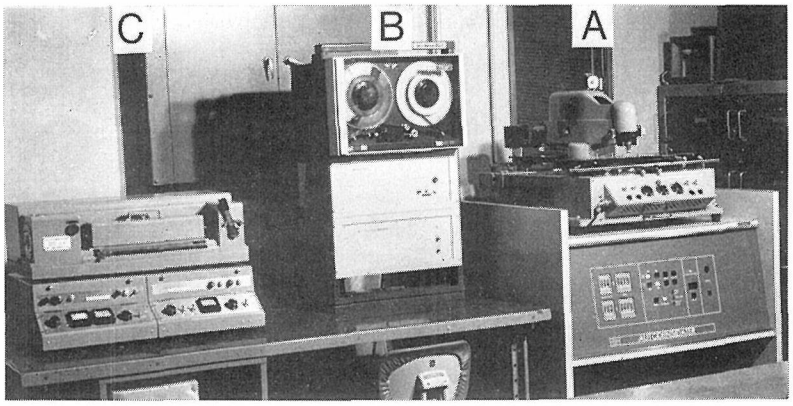

(a)

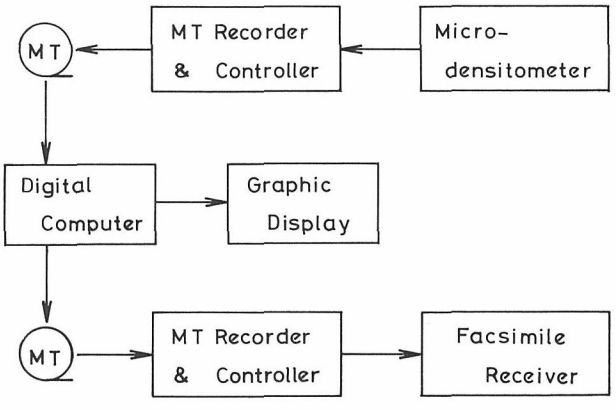

(b)

Fig. 2. Apparatus for digital image processing.
(a) General view.
A; Microdensitometer, B; Magnetic tape recorder and its controller, C; Facsimile receiver.
(b) Schematic flow of data.

F of lens L_d. The last lens L_i transforms this spectrum to an image. A photograph of the spectrum or image can be taken with a camera set in the plane F or in the image plane I. If a proper filter is set in the plane F, a processed image is formed in the plane I. This system is fixed on an iron timber (100 mm × 50 mm in cross section and 3000 mm long).

II.2 Digital Processing

An analogue processing method is insufficient to improve electron micrographic images up to the atomic order resolution, because of the degradation caused by a system itself as shown later in section IV.1. Thus an apparatus for digital image processing was constructed. A general view of this apparatus and a schematic flow of data are shown in Figs. 2(a) and 2(b).

The optical density distribution of an electron micrograph is measured automatically with a Joyce-Loebl double beam microdensitometer. Its sample stage is driven by programable stepping-motors in two independent (x, y) directions and the basic interval is 5 μm in each direction. Optical density in each image element, determined by a programed interval, is digitized by an analogue-to-digital converter within the microdensitometer. These digitized data have integral numbers between 0 and 999. With a magnetic tape (MT) recorder and its controller, a pack of 1024 digitized data in the x direction (y fixed) can be recorded in increasing order of y on MT for numerical processing by digital computer.

The data processed by computer are recorded on MT again and converted to analogue data by a digital-to-analogue converter within MT controller. These analogue data are displayed directly on a photographic paper with a facsimile receiver as a two-dimensional analogue picture. One picture element displayed with the facsimile receiver has a dimension of 0.193 mm × 0.215 mm, and the maximum number of picture elements is 970 in the x direction and 1200 in the y direction. Gray scale displayed with this apparatus is shown in Fig. 3. Although in this figure 20 levels are illustrated, actual pictures are to be displayed with 256 levels. It was confirmed that the image obtained with this system is practically same as the original one when no processing was made, as described in section IV.2.

III. THEORETICAL

An optical filtering system[8] is shown in Fig. 1(b). An electron micrograph of the amplitude transmittance $g_A(x, y)$ is set before the lens L_d in the object plane O and illuminated with a collimated laser beam. The amplitude distribution $G_A(\mu, \nu)$ in the back

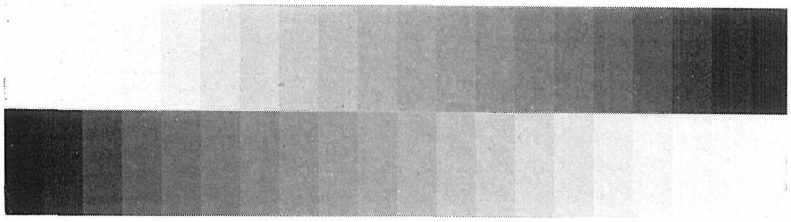

Fig. 3. Gray scale shows 20 discrete levels.

focal plane F of lens L_d can be expressed as

$$G_A(\mu, \nu)=\iint_{-\infty}^{+\infty} g_A(x, y) \exp\left[-2\pi i(\mu x+\nu y)\right] dxdy, \tag{1}$$

where the variables (μ, ν) and (x, y) are the spatial frequencies in Fourier space (plane F) and the position coordinates in the object plane O, respectively, and a constant phase factor is neglected. The physical meaning of Eq. (1) is that the lens L_d produces the Fourier transform of $g_A(x, y)$. After passing through the plane F the light waves form a real image in the plane I (*i.e.*, the lens L_i also produces the Fourier transform). When we take the coordinates (X, Y) in the image plane I to the opposite directions of (x, y) as shown in Fig. 1(b), then the amplitude distribution $\psi_A(X, Y)$ in the plane I is given by

$$\psi_A(X, Y)=\iint_{-\infty}^{+\infty} G_A(\mu, \nu) \exp\left[+2\pi i(X\mu+Y\nu)\right] d\mu d\nu=g_A(X, Y). \tag{2}$$

When we put a filter of the amplitude transmittance $T_A(\mu, \nu)$ in the plane F, the modified amplitude distribution $\psi_A'(X, Y)$ in the image plane I is written by

$$\begin{aligned}\psi_A'(X, Y)&=\iint_{-\infty}^{+\infty} G_A(\mu, \nu)\ T_A(\mu, \nu) \exp\left[+2\pi i(X\mu+Y\nu)\right] d\mu d\nu \\ &=g_A(X, Y) * t_A(X, Y),\end{aligned} \tag{3}$$

where $t_A(X, Y)$ is the Fourier transform of $T_A(\mu, \nu)$ and the $*$ denotes a convolution. The quantity $|\psi_A'(X, Y)|^2$ is the intensity distribution of a filtered image. This method is generally called *spatial frequency filtering*. When there exist both a periodic structure (*viz.* a lattice structure) and random noises caused by the photographic graininess in the electron micrograph of the amplitude transmittance $g_A(x, y)$, then $G_A(\mu, \nu)$ has not only sharp peaks in a discrete set of orders due to periodicity, but also some broad distribution due to noises. If we insert the filter grating $T_A(\mu, \nu)$ in the plane F which can let through the sharp peaks but block the rest of spectrum, the periodic structure will be enhanced with respect to the noise.

There is another method to remove random noises, called *linear integration*,[9] *i.e.*, the shifted superposition of the object picture with a period. Since the noises are regarded as random,[10] $\sqrt{N}$ improvement in the signal-to-noise ratio will be attained by this procedure, where N is the number of superposition.[11] These two methods are different in practice. In a special case, however, Hashimoto *et al.*[12] have shown that the optical image contrast formed by spatial frequency filtering using a filter grating is equivalent to the picture contrast by linear integration.

The principle of image processing is the same for optical and computer processing. The above procedures are followed in a computer for digital processing.

IV. RESULTS AND DISCUSSION

IV.1 Analogue Processing

A filter grating for optical filtering was made from a Fourier spectrum taken on a photographic film. It was an opaque mask with some pinholes which can let through only the sharp diffraction peaks due to periodicity in an electron micrograph, and this filter was inserted properly in the plane F in Fig. 1(b). The light waves passed through

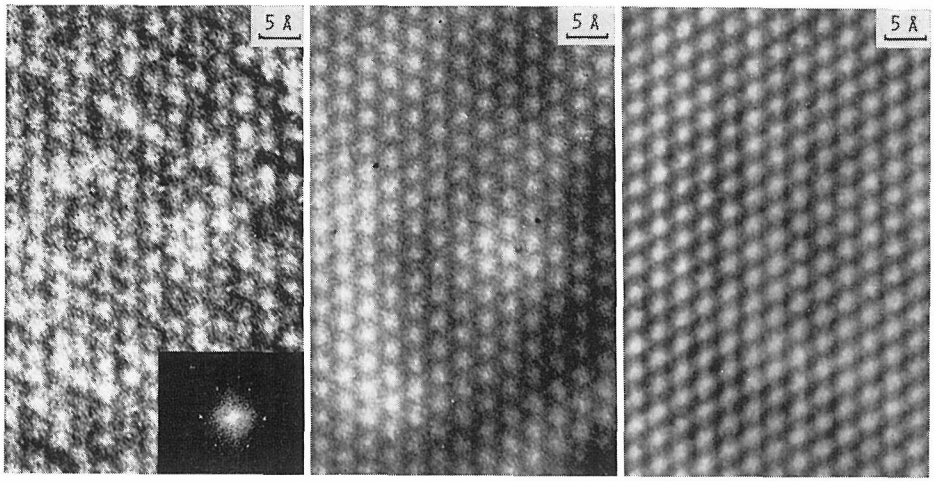

(a) (b) (c)

Fig. 4. High resolution electron micrograph of a thin crystalline film of cleaved molybdenite.
(a) MoS_2 networks taken at 500 kV (projected on the *ab*-plane). The insertion shows the optical diffraction pattern of the image. The filter was punched on the basis of this pattern. The diameter of pinholes was 2.0 mm for the central pinhole and 1.1 mm for others, corresponding to 1/8 $Å^{-1}$ and 1/15 $Å^{-1}$, respectively.
(b) Optically filtered image of (a).
(c) Photographically linear-integrated image of (a).

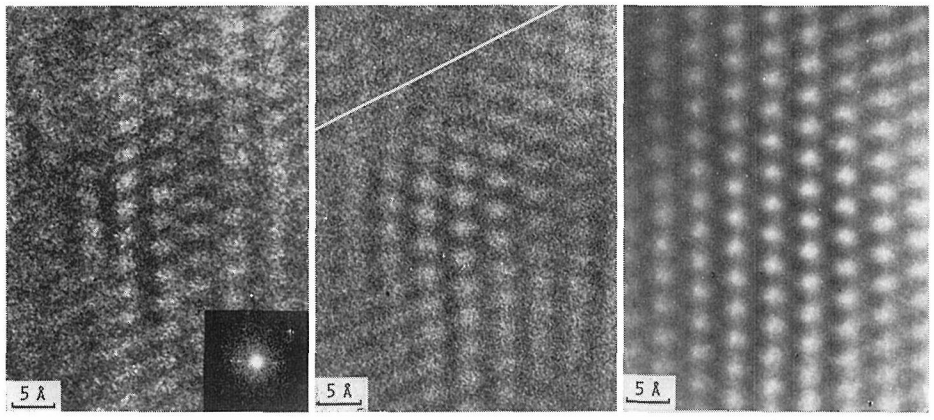

(a) (b) (c)

Fig. 5. High resolution electron micrograph of fibrous crystallite of vanadium oxide (Type F-2),[13] including lattice defects.
(a) V_2O_5 networks taken at 500 kV (projected on the *bc*-plane). The insertion shows the optical diffraction pattern. The pinhole diameter of the filter was 1.5 mm for the central pinhole and 2.0 mm otherwise, corresponding to 1/17 $Å^{-1}$ and 1/13 $Å^{-1}$, respectively.
(b) Optically filtered image of (a), which shows the half-period shifts of zig-zag layer lines along the oblique line more clearly than (a).
(c) Photographically linear-integrated image of (a).

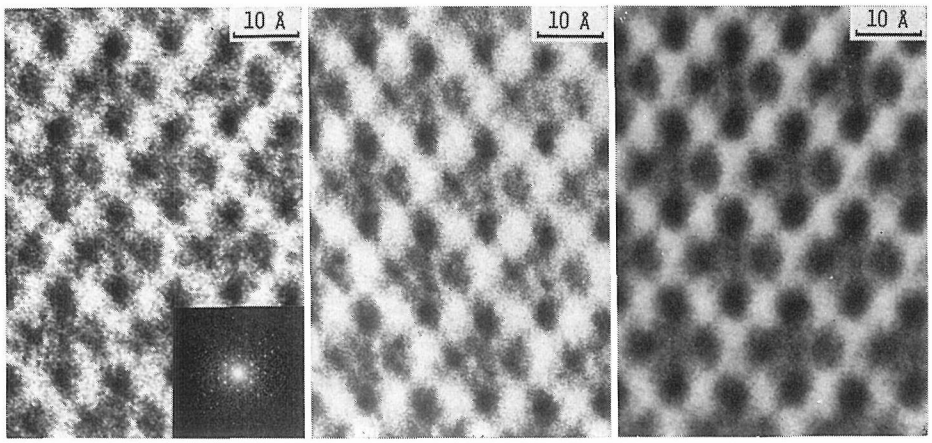

(a) (b) (c)

Fig. 6. High resolution molecular images of hexadecachloro-Cu-phthalocyanine in a thin crystalline film.
(a) Molecular images taken at 500 kV (projected along the *c*-axis). The insertion shows the optical diffraction pattern. The pinhole diameter of the filter was 1.0 mm for all, corresponding to 1/36 $Å^{-1}$.
(b) Optically filtered image of (a).
(c) Photographically linear-integrated image of (a).

this filter and formed an image. The periodic structure in the electron micrograph was thus enhanced against the noise. The random noise removal in an electron micrograph was performed also by photographic linear integration (*viz.*, a multiple exposure technique combined with the periodic translation by using a conventional enlarger). The linear integration method gives better results than optical filtering in the signal-to-noise ratio. Examples of these two processing methods are shown in Figs. 4, 5, and 6. The size of pinholes used in optical filtering is shown in the caption of each figure. Since the filter has pinholes of finite size, the surrounding region of each diffraction peak as well as the peak itself is allowed to pass through. Figure 5(a) is the high resolution lattice image including a lattice defect, and optical filtering can reproduce the lattice defect in a filtered photograph as shown in Fig. 5(b). The filtering method also reproduces a large scale pattern more faithfully as seen in Fig. 4(b) which corresponds to light and dark areas of the original micrograph (Fig. 4(a)). Thus the filtering method is more adequate to reduce random noises when both the periodic and the large scale irregular structures should be reproduced in processed images. The linear integration procedure, however, is not adequate to apply to the irregular structures (see Fig. 5).

Several technical problems still exist in the optical filtering method. For example the multiple reflection of light between lenses causes the interference effect on the image.

IV.2 Digital Processing

Spatial frequency filtering and linear integration were carried out with the digital processing system, including a FACOM 230-48 computer in our Institute. The FORTRAN program was written by applying the Cooley-Tukey's fast Fourier transform (FFT) algorithm[14] which was available from the FACOM Scientific Subroutine Library. The high resolution electron micrograph of hexadecachloro-Cu-phthalocyanine molecular

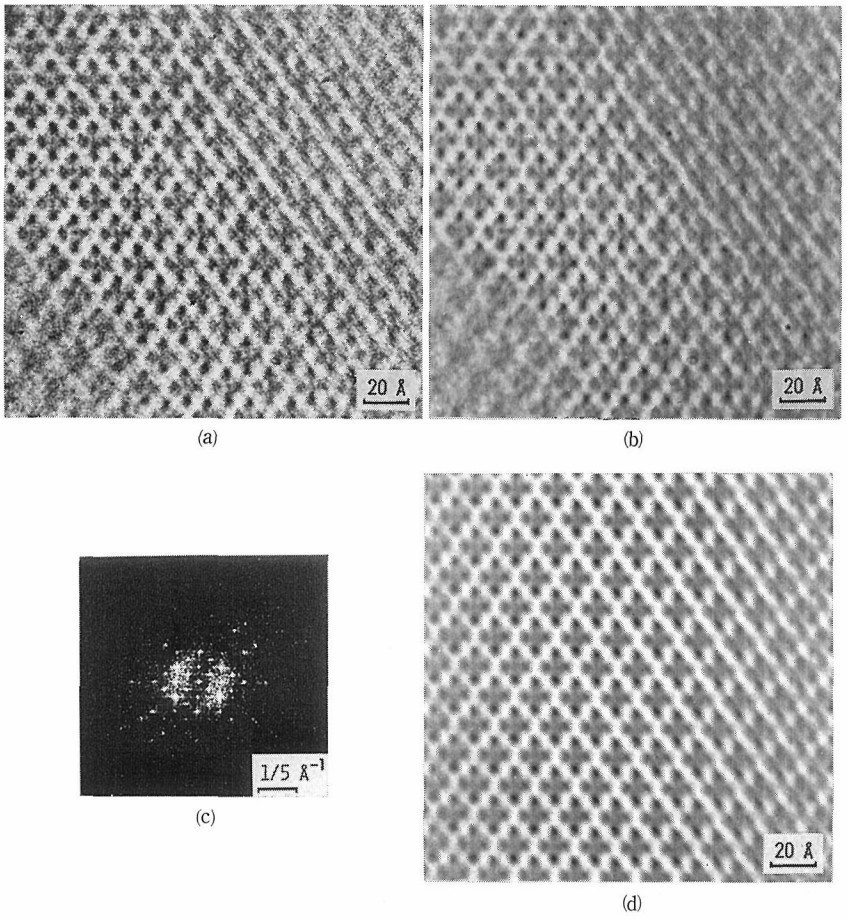

Fig. 7. Spatial frequency filtering by computer.
(a) Molecular images of hexadecachloro-Cu-phthalocyanine.
(b) Picture displayed with the facsimile receiver without any processing.
(c) Fourier spectrum of (b), displayed on the graphic display device.
(d) Filtered picture of (b).

images (Fig. 7(a)) was chosen as one to be processed. The optical density distribution of the electron micrograph was measured by a 10 μm interval (corresponding to 0.7 Å on the micrograph) in each direction and with a receiving slit (440 μm $\times$ 440 μm, corresponds to 10 μm $\times$ 10 μm on the sample stage). The 256 $\times$ 256 original matrix of recorded digital data was displayed with the facsimile receiver without any processing (see Fig. 7 (b)). Figures 7(a) and 7(b) show that our apparatus can reproduce the correct optical density distribution of an electron micrograph.

The Fourier transformation of the original matrix of data was executed by the FFT program, and Fig. 7(c) shows the Fourier spectrum displayed on a graphic display device (a storage-type CRT) connected directly to the computer. The pattern of this spectrum is same as the optical diffraction pattern (the insertion of Fig. 6(a)) as expected, and shows strong diffraction spots due to periodicity. Spatial frequency filtering was performed according to the way described in Chap. III, and the result is shown in Fig. 7(d). The filter function of this filtering was equal to 1 for the central positions of sharp diffraction

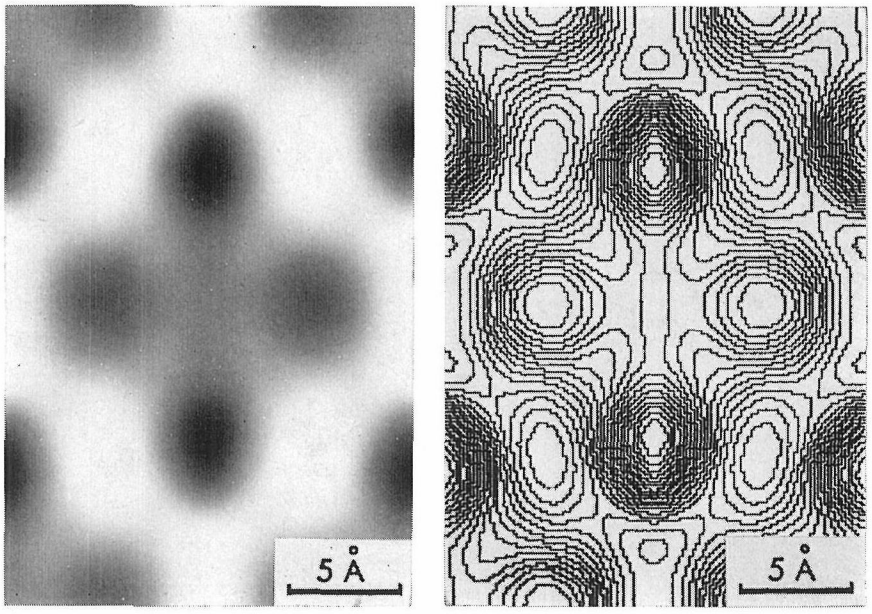

(a) (b)

Fig. 8. Unit cell image obtained by spatial frequency filtering by computer.
(a) Displayed with the facsimile receiver.
(b) Equidensity map corresponding to (a) with 20 contour lines on the graphic display device.

peaks, and 0 otherwise. A single averaged unit cell was displayed with the facsimile receiver (see Fig. 8(a)). Figure 8(b) on the graphic display device is the equidensity map with 20 contour lines corresponding to Fig. 8(a). The equidensity map shows the shape of a molecular image more distinctly.

Linear integration was undertaken by the computer, and 27 unit cells with well-shaped molecular image in Fig. 7(b) were superposed. The cross-correlation:

$$F(X,\ Y)=\iint A(x,\ y)\ B(X+x,\ Y+y)\ dxdy, \tag{4}$$

is calculated in order to determine a proper location for superposition. Here A and B denote two molecular images. The quantity $F(X,\ Y)$ is considered as an index of pattern recognition. The actual procedure of this calculation is as follows: (1) A sample area which contains an image of one molecule is chosen as a reference area, and the image is represented by $m\times n$ density matrix whose elements are denoted by $a_{ij}(i=1,\ 2,\ \ldots,\ m$ and $j=1,\ 2,\ \ldots,\ n)$. (2) A tentative origin $(X_0,\ Y_0)$ of another molecular image is assumed on the basis of the lattice constants obtained from Fig. 7(c). (3) The origin $(X,\ Y)$ is varied within the searching area around $(X_0,\ Y_0)$, and the following quantity is calculated for each $(X,\ Y)$:

$$F(X,\ Y)=\sum_{i}^{m}\sum_{j}^{n} a_{ij}\ b_{ij}. \tag{5}$$

Here b_{ij} denotes the element $(i,\ j)$ of the $m\times n$ matrix and is determined by assuming $(X,\ Y)$ as the origin. (4) The exact location of superposition is fixed at the point $(X_M,$

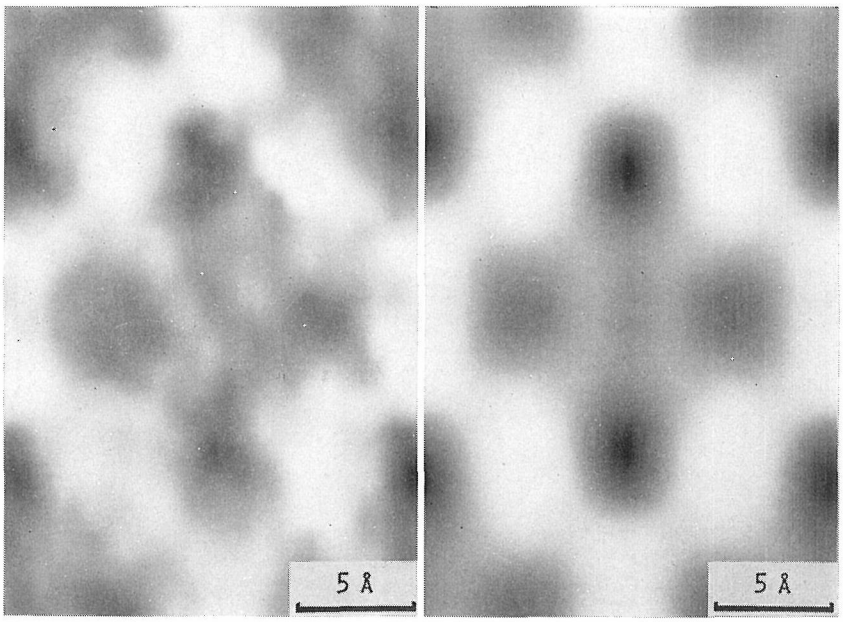

(a) (b)

Fig. 9. Linear integration by computer.
(a) Unit cell image sampled from Fig. 7(b).
(b) Resulting image of linear integration (27 times).

Y_M) where $F(X, Y)$ attains its maximum, and the corresponding matrix to this origin (X_M, Y_M) is added to the original reference matrix. (5) Using this result of superposition as a new reference matrix, the whole procedure is repeated for other molecular images.

The final result of linear integration is shown in Fig. 9(b), and the signal-to-noise ratio is improved as in the case of spatial frequency filtering (see Fig. 8(a)). Apart from the results of optical processing, the almost same results are obtained by linear integration or spatial freqency filtering in computer processing. This can be interpreted that sharper pinholes were used for filtering by computer than for optical filtering, and the result of spatial frequency filtering is equivalent to that of linear integration, as expected theoretically.

V. CONCLUSION

Computer and optical image processing systems were constructed and applied to removing random noises in EM images. Spatial frequency filtering and linear integration in these systems have improved the signal-to-noise ratio in the original electron micrographs which possess both periodic structures and random noises. When a lattice defect exists in the high resolution lattice image (see Fig. 5), the defect is reproduced by simple optical filtering. Spatial frequency filtering will be useful if both the periodic and the large scale irregular structures should be reproduced in processed images.

ACKNOWLEDGMENT

The authors would like to acknowledge Professor N. Uyeda and Mr. Y. Fujiyoshi, Kyoto University, for their allowance to use a high resolution electron micrograph of vanadium oxide. The authors are grateful to the staff of the Computer Center in this Institute, for the provision of computing facilities. Thanks are due to Dr. K. Kajiwara in the preparation of this paper.

REFERENCES

(1) O. Scherzer, *J. Appl. Phys.*, **20**, 20 (1949).
(2) K. Kobayashi, E. Suito, N. Uyeda, M. Watanabe, T. Yanaka, T. Etoh, H. Watanabe, and M. Moriguchi, Abstracts, 8th International Congress on Electron Microscopy, Canberra, 1974, p. 30.
(3) F. C. Billingsley, *Appl. Optics*, **9**, 289 (1970).
(4) A. Klug and D. J. DeRosier, *Nature*, **212**, 29 (1966).
(5) G. W. Stroke and M. Halioua, *Optik*, **35**, 50 (1972).
(6) J. Frank, *Biophys. J.*, **12**, 484 (1972).
(7) C. A. Taylor and H. Lipson, "Optical Transforms", G. Bell and Sons, London, 1964.
H. Lipson Ed., "Optical Transforms", Academic Press Inc., London and New York, 1972.
(8) E. L. O'Neill, *I.R.E. Trans. Inf. Theory*, **IT-2**, 56 (1956).
(9) R. Markham, J. H. Hitchborn, G. J. Hills, and S. Frey, *Virology*, **22**, 342 (1964).
(10) R. C. Valentine in "Advances in Optical and Electron Microscopy", Vol. 1, R. Barer and V. E. Cosslett Ed., Academic Press, London and New York, 1966, p. 180.
(11) R. Nathan in "Advances in Optical and Electron Microscopy", Vol. 4, R. Barer and V. E. Cosslett Ed., Academic Press, London and New York, 1971, p. 85.
(12) H. Hashimoto, E. Endoh, and T. Tanji, Abstracts, US-Japan Seminar on HVEM, Honolulu, 1976.
(13) N. Uyeda, Y. Fujiyoshi, and K. Ishizuka, *ibid.*, 1976.
Y. Fujiyoshi, K. Ishizuka, and N. Uyeda, *J. Electron Microsc.*, **26**, 47 (1977).
(14) J. W. Cooley and J. W. Tukey, *Math. Comput.*, **19**, 297 (1965).